



저작자표시-비영리-변경금지 2.0 대한민국

이용자는 아래의 조건을 따르는 경우에 한하여 자유롭게

- 이 저작물을 복제, 배포, 전송, 전시, 공연 및 방송할 수 있습니다.

다음과 같은 조건을 따라야 합니다:



저작자표시. 귀하는 원저작자를 표시하여야 합니다.



비영리. 귀하는 이 저작물을 영리 목적으로 이용할 수 없습니다.



변경금지. 귀하는 이 저작물을 개작, 변형 또는 가공할 수 없습니다.

- 귀하는, 이 저작물의 재이용이나 배포의 경우, 이 저작물에 적용된 이용허락조건을 명확하게 나타내어야 합니다.
- 저작권자로부터 별도의 허가를 받으면 이러한 조건들은 적용되지 않습니다.

저작권법에 따른 이용자의 권리는 위의 내용에 의하여 영향을 받지 않습니다.

이것은 [이용허락규약\(Legal Code\)](#)을 이해하기 쉽게 요약한 것입니다.

[Disclaimer](#)

이학석사 학위논문

Multi-Stacked Graphene Pellicle
for Extreme Ultra Violet
Lithography

극자외선 노광 기술용 적층 그래핀 펠리클

2019 년 8 월

서울대학교 대학원
화학부 물리화학 전공
김 은 정

Multi-Stacked Graphene Pellicle for Extreme Ultra Violet Lithography

극자외선 노광 기술용 적층 그래핀 펠리클

지도 교수 홍 병 희

이 논문을 이학석사 학위논문으로 제출함
2019 년 8 월

서울대학교 대학원
화학부 물리화학 전공
김 은 정

김은정의 이학석사 학위논문을 인준함
2019 년 8 월

위 원 장 _____ 이 정 호 (인)

부위원장 _____ 홍 병 희 (인)

위 원 _____ 송 윤 주 (인)

Abstract

Multi-Stacked Graphene Pellicle for Extreme Ultra Violet Lithography

Eun Jung Kim

Physical Chemistry, Department of Chemistry

The Graduate School

Seoul National University

As the technology of integrated circuits develops, it is inevitable to reduce the line width of transistors. In order to reduce the line width, it is necessary to develop various semiconductor processing technologies, among which exposure technology has particularly attracted attention. The deep ultraviolet (DUV) lithography techniques using wavelengths on the order of a few hundred nanometers have reached their limits. And the introduction of extreme ultraviolet (EUV) lithography techniques using a lower wavelength range as a new technology has begun. [1~2] In this case, the light in the EUV region of 13.5 nm wavelength is emitted from the high-density plasma. Thus, the process must be performed in a vacuum environment unlike the conventional DUV lithography. These differences not only require new optical systems, but also require the development of reticle materials, including pellicles. [3~10]

In this thesis, we propose 'Multi-Stacked Graphene Pellicle' for EUV lithography. Graphene, which is a carbon isotope and has a sp^2 hybridized structure in a two-dimensional plane has excellent properties, because it has a thickness of a

single layer of atoms. [11-12] Among them, the reason that can be applied to the pellicle for EUV lithography is that it is excellent in electrical characteristics, thermal properties, optical properties and mechanical strength.

Before the proposal of ‘Multi-Stacked Graphene Pellicle’, a large area graphene film was synthesized by chemical vapor deposition (CVD) method. By the vapor-phase molecular doping and its characteristics can be controlled in a better direction. We also propose a novel transfer method, paraffin-assisted transfer. This method can achieve graphene with better characteristics than conventional transfer method.

The proposed ‘Multi-Stacked Graphene Pellicle’ for EUV lithography must be developed in terms of heat load, transmittance in EUV region and productivity. To meet these requirements, we aimed to develop thin films of several tens of nanometer. The typical wet transfer method was repeated to prepare multi-stacked graphene film corresponding to 10 (ten) layers. UV-Vis and Raman spectroscopic analysis showed that the transfer and stacking process was completed properly. The thickness of multi-stacked graphene film was measured by atomic force microscope (AFM). And the result was about 15.4 nm. To measure the transmittance in the EUV region multi-stacked graphene film, a free-standing sample of 10 mm in diameter was fabricated. And the EUV light transmittance was in a vacuum environment 87 %.

Keyword: EUV, Multi-Stacked Graphene Pellicle, EUV transmittance, CVD, paraffin-assisted transfer method

Student Number: 2017-29383

Table of Contents

Abstract	i
Table of Contents	iii
List of Tables	v
List of Figures	vi
Chapter 1. Introduction	1
1.1. Motivation	1
1.2. Outline of the Thesis	2
Chapter 2. CVD Graphene Films	4
2.1. Synthesis of CVD Graphene Films	4
2.2. Modulation of Properties of Graphene	9
Chapter 3. Paraffin-assisted Graphene Transfer	1 3
3.1. Introduction	1 3
3.2. Experimental	1 6
3.3. Results and Discussion	1 8
Chapter 4. Multi-Stacked Graphene Pellicle for Extreme Ultra Violet Lithography	1 9

4.1. Introduction	1 9
4.2. Experimental	2 1
4.3. Results and Discussion	2 6
Chapter 5. Conclusion	3 0
Bibliography	3 1
국 문 초 록	3 5

List of Tables

Chapter1. Introduction

Table 1.1. Comparison of lithographic features and tools between ArF and EUV

Chapter2. CVD Graphene Films

Table 2.1. The properties of linear aliphatic diamines.

List of Figures

Chapter1. Introduction

Fig. 1.1. Annual data growth trend. Data growth will grow from 33 ZB in 2018 to 175 ZB by 2025.

Chapter2. CVD Graphene Films

Fig. 2.1. Growth mechanism of graphene in CVD process.

Fig. 2.2. CVD system for graphene synthesis.

Fig. 2.3. Schematic illustrations of Graphene FETs fabrication. (a) Preparation of target substrate, (b) Electrode (Au/Ti) deposition by thermal evaporation, (c) Graphene films transfer by any transfer method, (d) Isolation of graphene films by E-beam lithography.

Fig. 2.4. Characterization of single layer graphene. (a) Optical microscopy image of graphene film on SiO₂/Si substrate. (b) Raman spectra (514 nm laser excitation wavelength) for graphene transfer onto SiO₂/Si substrate. (c) Current-voltage characteristics of graphene FET.

Fig. 2.5. Raman spectra of graphene doped with aliphatic diamine. (a) G peak position for pristine and doped graphene, (b) 2D peak position for pristine and doped graphene

Fig. 2.6. Current-voltage transfer characteristics of graphene doped with aliphatic diamines. (a) Current-voltage characteristics by diamine type, (b) current-voltage characteristics by doping time

Chapter3. Paraffin-assisted Graphene Transfer

Fig. 3.1. Schematic illustrations of the Paraffin-assisted Graphene Transfer process. (a) Paraffine wax was melted on graphene/Cu, (b) the copper was removed by APS etchant, (c) paraffine-assisted graphene was transferred onto target substrate, (d) paraffin was removed by using toluene.

Fig. 3.2. Optical microscope image of the graphene film with paraffin removed after attachment at various temperature.

Fig. 3.3. Comparison of Raman spectra for graphene transferred onto the SiO₂/Si substrate. (a) Representative Raman spectra of graphene transferred by paraffin, (b) G peak position, (c) 2D peak position, (d) 2D peak position versus G peak position, (e) 2D peak position versus I_{2D}/I_G ratio.

Chapter4. Multi-Stacked Graphene Pellicle for Extreme Ultra Violet Lithography

Fig. 4.1. Chip Scale-down and lithography wavelength. The light source used in the 2010s is ArF-immersion at 193 nm wavelength, and A new technology, EUV, uses a wavelength of 13.5 nm.

Fig. 4.2. Schematic of EUV lithography system. Light sources delivering hundreds of watts to wafer. Lithography optics focus the reflected light onto a chip. Schematically simple, but real systems are large and complex.

Fig. 4.3. Schematic of the graphene stacking process. Multi-stacked graphene film was made by conventional wet transfer method on the CVD graphene.

Fig. 4.4. Fabrication process of free-standing sample. (a) Removal of PMMA by using toluene at clean and stable room. The sample was soaked vertically and then held up and dried. (b) a 15.4 nm thickness free-standing multi-stacked graphene film with inner diameter of 10 mm.

Fig. 4.5. Transmittance at visible light, thickness of multi-stacked graphene film. (a) Visible light transmittance of 1 layer (1L), 7 layer (7L) and 10 layer (10L) graphene films. (b) Height data of multi-stacked (10L) graphene film measured by AFM. The median thickness of 10L graphene is 15.4 nm.

Fig. 4.6. Raman spectra for graphene and multi-stacked graphene onto the SiO₂/Si substrate. (a) Representative Raman spectra of 1 layer, 7 layer and 10 layer graphene film (b) G peak position, (c) 2D peak position, (d) 2D peak position versus G peak position, (e) 2D peak position versus I_{2D}/I_G ratio.

Fig. 4.7. EUV transmission characteristics of multi-stacked graphene film.

(a) Reference light on CCD, (b) light transmitted through the sample on CCD. EUV transmittance (87 %) of a multi-stacked graphene sample was obtained by comparing (a) and (b). (scale bar = 1 mm).

Chapter 1. Introduction

1.1. Motivation

With the advent of advanced technology including 5G, artificial intelligence (AI), internet of thing (IoT) and automatic driving, the amount of data used in our lives has increased tremendously. Looking at worldwide data growth, data growth is expected to increase from 33 ZB in 2018 to 175 ZB in 2025. (Fig. 1.1.) This also means that the integrated circuit (IC) market is still on. Scaling down the size of a transistor in an IC was inevitable depending on the times. Scaling down requires the development of various semiconductor process technologies. Among them, the semiconductor industry is paying attention to the development of lithography technology. Now that we have reached the limits of deep ultraviolet (DUV) lithography, the introduction of extreme ultraviolet (EUV) lithography using a lower wavelength band as a new technology has begun.

EUV lithography is a lithography technique using very short wavelength (13.5 nm) light called extreme ultraviolet ray. This technique enables fine pattern processing that could not be patterned in lithography technology using conventional ArF excimer laser light. As shown in Table 1.1., ArF-immersion which are conventional technologies and EUV differ not only in wavelength but also in the system configuration. EUV light is emitted from a high-density plasma and is absorbed in the air, so exposure proceeds in a vacuum environment. These differences not only require new optical systems, but also require the development of reticle materials including pellicles. [3-4]

The pellicle is a component of a reticle, which prevents contamination on the front of the mask. A thin film having high transmittance is located at a distance from the mask surface. Pellicle is a necessary component because contamination of the mask causes wafer failure. Pellicle is a necessary component because contamination of the mask causes wafer failure. There are requirements for the EUV pellicle. High transmittance is required due to the optical system using reflection as well as the absorption characteristics of the EUV wavelength. (Fig. 1.2.) In addition, the film must have immunity to the thermal load caused by the high energy of the EUV light. To meet the above-mentioned requirements, a thin film having a thickness of several tens of nanometers is proposed. The proposed pellicle film should be stand-alone in full size ($132 * 104 \text{ mm}^2$) and productive.

1.2. Outline of the Thesis

In this thesis, a ‘Multi-Stacked Graphene Pellicle’ is proposed, which can be generally applied to EUV lithography used in very-large-scale integration (VLSI). Since graphene has outstanding electrical and optical properties, this is possible proposal. First, multi-stacked graphene film is fabricated from CVD graphene films and characterized. Various methods such as Raman, AFM and UV-Vis are used to analyze the characteristics of the stacked graphene. Subsequently, a free-standing sample with a thickness of 15.4 nm is fabricated to measure the transmittance at 13.5 nm wavelength. The possibility of applying EUV pellicle of multi-stacked graphene film is examined through a series of procedures.

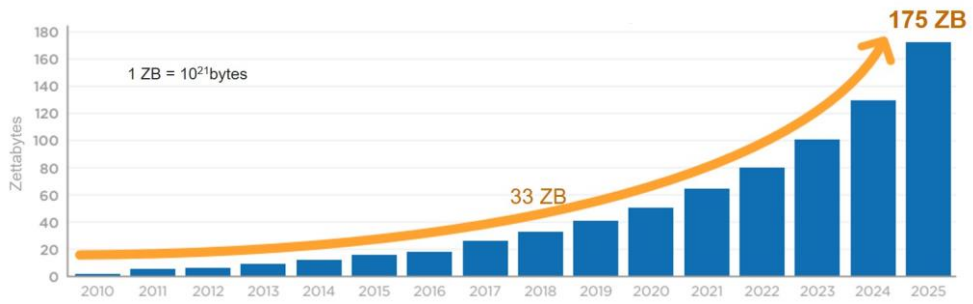


Fig. 1.1. Annual data growth trend. Data growth will grow from 33 ZB in 2018 to 175 ZB by 2025. Adapted from *Data Age 2025, IDC/Seagate, 2018*.

	ArF-immersion	EUV
Wavelength	193 nm	13.5 nm
Resolution	66 nm	20 nm
Source	ArF Laser	EUV Plasma
Optics	Lens	Mirror
Mask	Transmission	Reflection

Table 1.1. Comparison of lithographic features and tools between ArF and EUV.

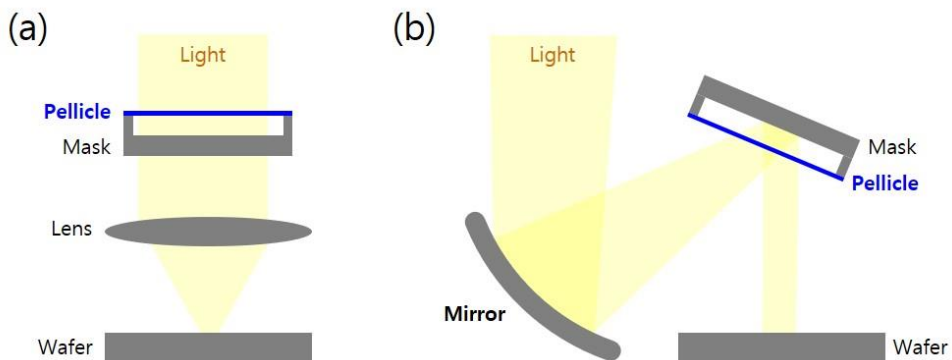


Fig. 1.2. Schematic illustrations of lithography system. (a) Conventional lithography, (b) EUV lithography.

Chapter 2. CVD Graphene Films

2.1. Synthesis of CVD Graphene Films

In laboratory scale graphene research, CVD is a widely used process for fabricating uniform and high-quality graphene films. [13-14] Since this process is cost-effective, it is also advantageous for mass production of graphene films. In a CVD process, a substrate is exposed to volatile precursors. Then, the decomposed precursor reacts on the surface of the substrate to produce a target material. (Fig. 2.1.) Major factors are controlled to fabricate the desired composition of material in the CVD process. These factors are equipment, process type and process conditions (e.g., temperature, pressure and gas flow).

The first synthesis of graphene in the CVD process was the synthesis of few-layer graphene (FLG) on a nickel sheet. [15] And thereafter a method of growing graphene films on various metal substrate such as Cu and Ni has been reported. [16-17] In the case of metal with low carbon solubility such as copper, it is grown due to surface adsorption and more regular graphene film is obtained. Therefore, Cu foil is used for large area synthesis. The graphene films synthesized in this way have uniform electrical and mechanical properties as compared with the samples in the exfoliation method. For the precursors, various carbon sources have been investigated improve the quality of the graphene film. The most widely used precursor is methane and a high temperature process is required for dissociation of this carbon source. [18]

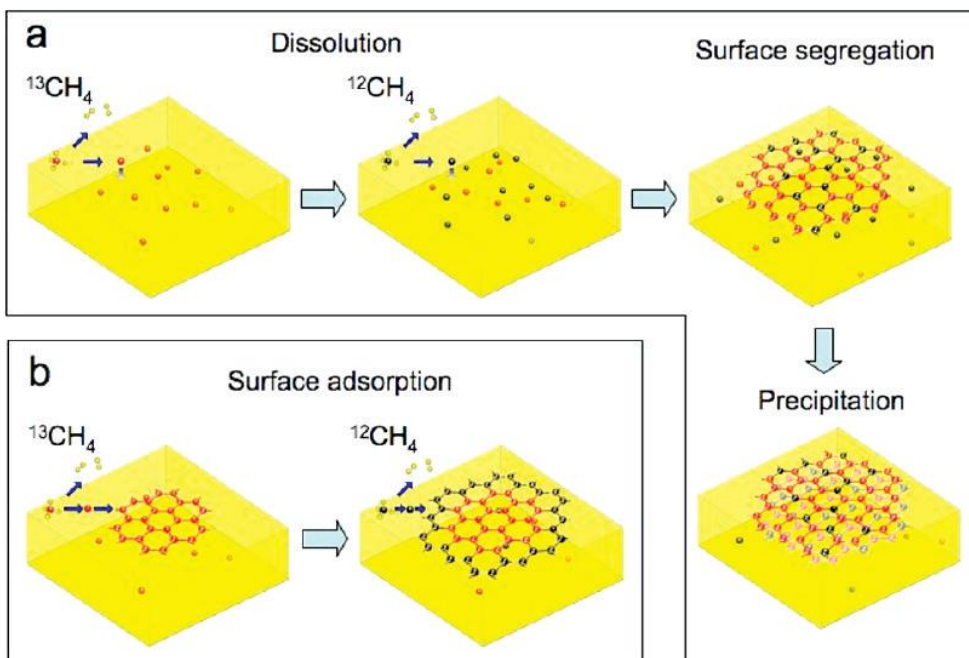


Fig. 2.1. Growth mechanism of graphene in CVD process. [18]

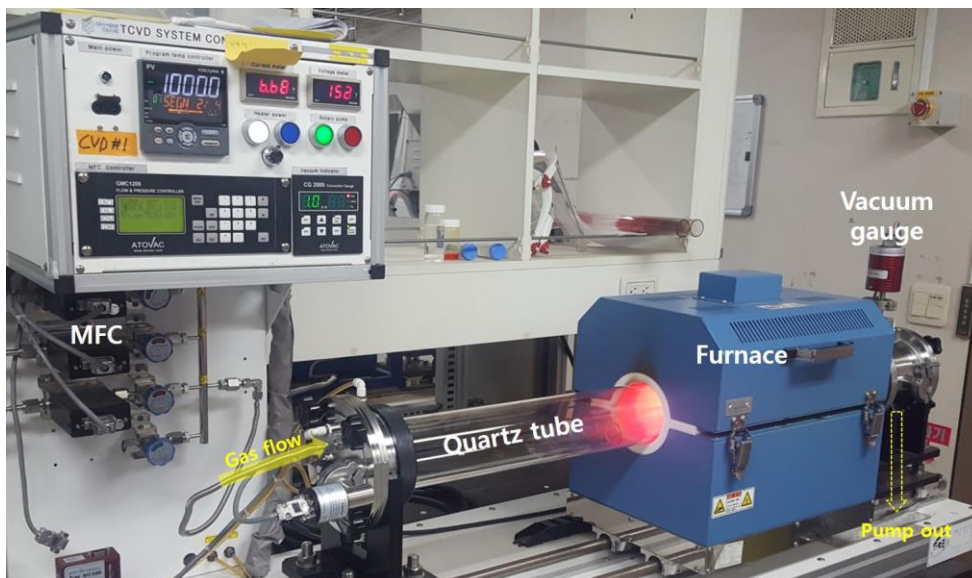


Fig. 2.2. CVD system for graphene synthesis.

Synthesis of CVD Graphene. Graphene was grown on polycrystalline Cu foil (99.7 %) with hydrogen (15 sccm) and methane (100 sccm) for 30min at 1000°C under low pressure (0.76 Torr) in a quartz tube. The annealing time including temperature rise was 1 hour under hydrogen (15 sccm). After the growth time, the furnace was cooled down to room temperature with hydrogen (15 sccm). The graphene on frontside of Cu foil was coated with Poly (methyl methacrylate) (PMMA, $(C_5O_2H_8)_n$) and the graphene on backside was etched by oxygen reactive ion etching (RIE). The Cu foil was removed by Cu etchant (0.1 M ammonium persulfate). For analysis, the graphene floating on deionized water was transferred to a substrate such as silicon wafer, and then PMMA was removed with acetone.

Graphene field effect transistor (FET) fabrication. Fig. 2.3 represents the overall process of manufacture. Au 500 Å/ Ti 50 Å were deposited on the silicon substrate as an electrode. Thermal evaporation was used as a deposition method, and a patterned electrode was formed using a patterned shadow mask. The graphene was transferred onto the substrate having electrodes formed thereon by a wet transfer method. After the transfer process, E-beam lithography was performed for isolated transistor formation.

Characterization of single layer graphene. Fig. 2.4a shows optical microscopy images of the transferred graphene on SiO₂/Si substrate. The continuous graphene films were transferred with contamination and polymer residue. These are related to peak position shifts observed in Raman spectra. The residues of PMMA that are incompletely removed are observed and lead to surface contamination.

Typical Raman spectra of graphene shows D, G and 2D peak at 1350, 1580 and 2680 cm^{-1} . [19] We have also identified unique peaks in our experiments, as seen in Fig. 2.4b. G peak was identified at 1589 cm^{-1} which shifted from the typical peak position, due to the PMMA residue effect used in the transfer process. (Fig. 2.4b)

Analysis of the current-voltage characteristics measured by the Graphene FET shows the same result. This device replaces only silicon channels with graphene in common transistors. A typical Graphene FET has a dirac point near 0 V [20], but our transistor has a dirac point near 20 V. (Fig. 2.4c) The shift of the Dirac point is due to graphene doping and is p-doped from its position. [21]

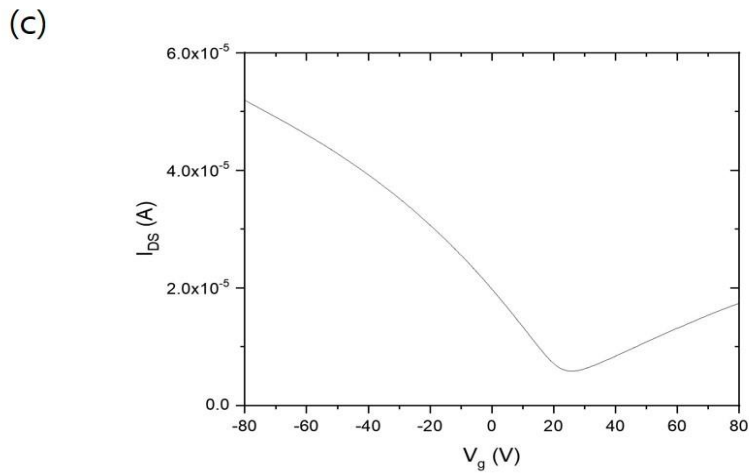
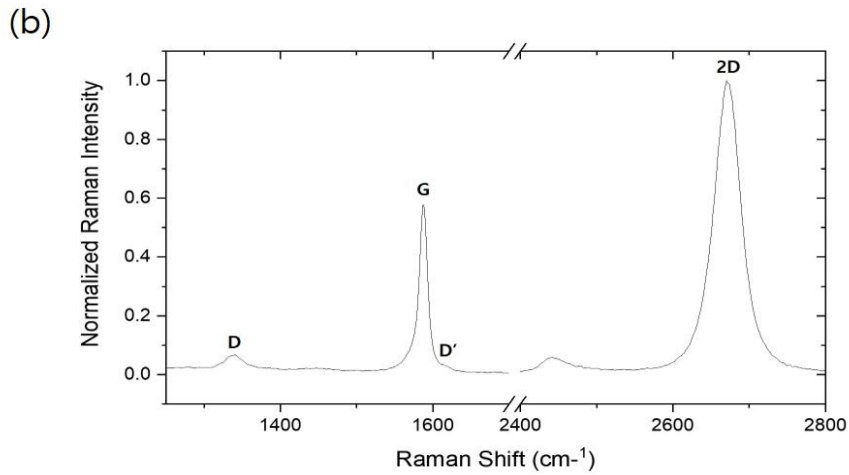
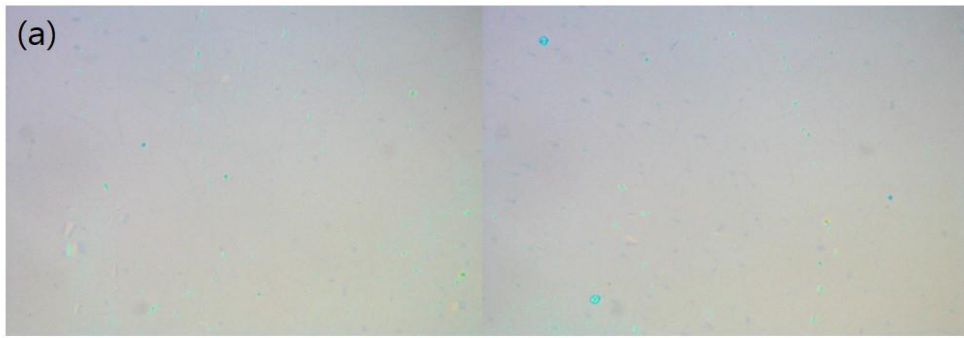


Fig. 2.4. Characterization of single layer graphene. (a) Optical microscopy image of graphene film on SiO₂/Si substrate. (b) Raman spectra (514 nm laser excitation wavelength) for graphene transfer onto SiO₂/Si substrate. (c) Current-voltage characteristics of graphene FET.

2.2. Modulation of Properties of Graphene

Recent advances in mass production of graphene films have focused on improving the properties of graphene. The goal of these efforts is to fabricate sustainable, controllable and high-quality graphene films. Especially, Doping is an effective way to tune the band-gap of graphene, including substitutional atomic doping by reactive gases, electrical/electrochemical doping by applying gate bias and chemical doping by acids or reducing/oxidizing agent. In graphene research, the chemical doping is a widely used technique because of its simplicity and strong doping strength, where the doping effect is obtained by electron transfer between graphene and dopants. Therefore, the charge transfer capability of its functional groups and the molecular structure must be taken into consideration for more effective doping. [21-23]

Vapor-Phase Molecular Doping. A single layer graphene was synthesized by chemical vapor deposition (CVD) at 1,000 °C and n-doped by vapor phase molecular doping at 70 °C. To demonstrate a stable n-doped graphene and to find out how the molecular structure of the dopant affects its strength and stability, we selected linear aliphatic diamines as dopants. The selected diamines are ethane-1,2-diamine (EDA), propane-1,3-diamine (PDA), butane-1,5-diamine (BDA) and Hexane-1,6-diamine (HDA). Table 2.1. shows the properties of linear aliphatic diamines.

Characterization of single doped graphene. Raman spectroscopy was used to analyze doping level, and electrical properties were measured by field effect transistors.

	Name	M_w (g/mol)	T_m (°C)	T_f (°C)	T_b (°C)
2 carbons	Ethane-1,2-diamine	60.10	10	38	117
3 carbons	Propane 1,3-diamine	74.12	-12	51	140
4 carbons	Butane-1,4-diamine	88.15	25~28	51	158
6 carbons	Hexane-1,6-diamine	116.20	42~45	80	204

Table 2.1. The properties of linear aliphatic diamines.

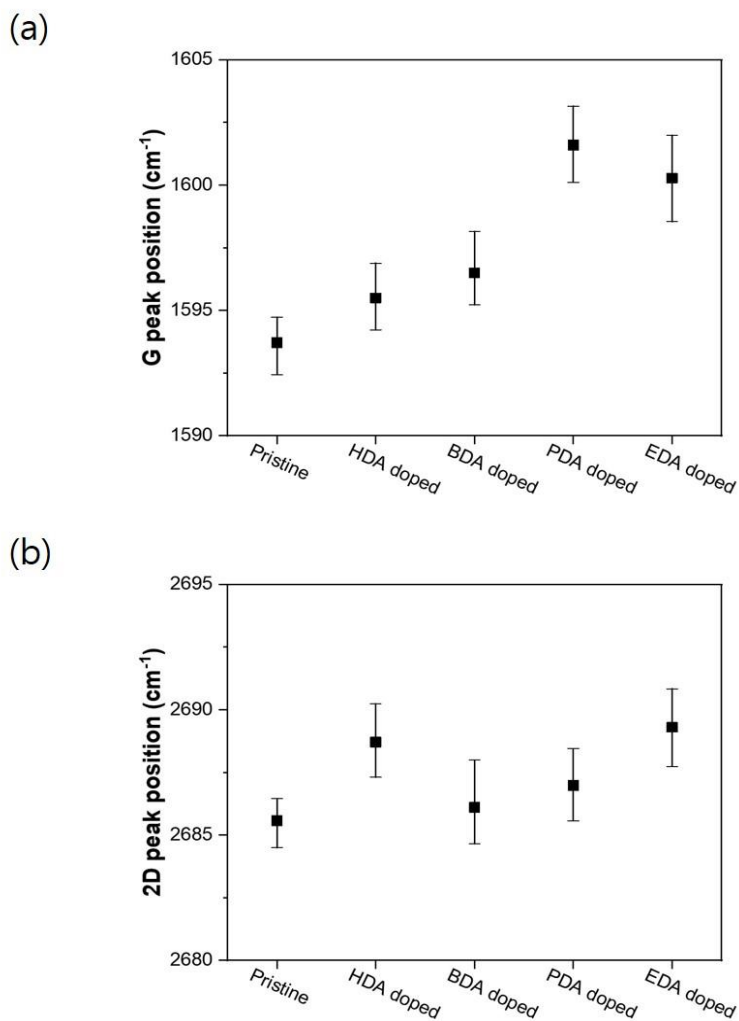


Fig. 2.5. Raman spectra of graphene doped with aliphatic diamine. (a) G peak position for pristine and doped graphene, (b) 2D peak position for pristine and doped graphene.

The results show that the longer carbon chain of a diamine molecule reduces the electron transfer per unit area of graphene, resulting in the decrease in n-doping effect, while the doping stability increases as molecular weight increases. Since the diamines are linear aliphatic compounds, the amine groups always have different orientations depending on the length of the carbon chains. Our study supports that the vapor phase doping is an effective route to optimize the orientation of the dopant molecules for enhanced stability and stronger doping of graphene films.

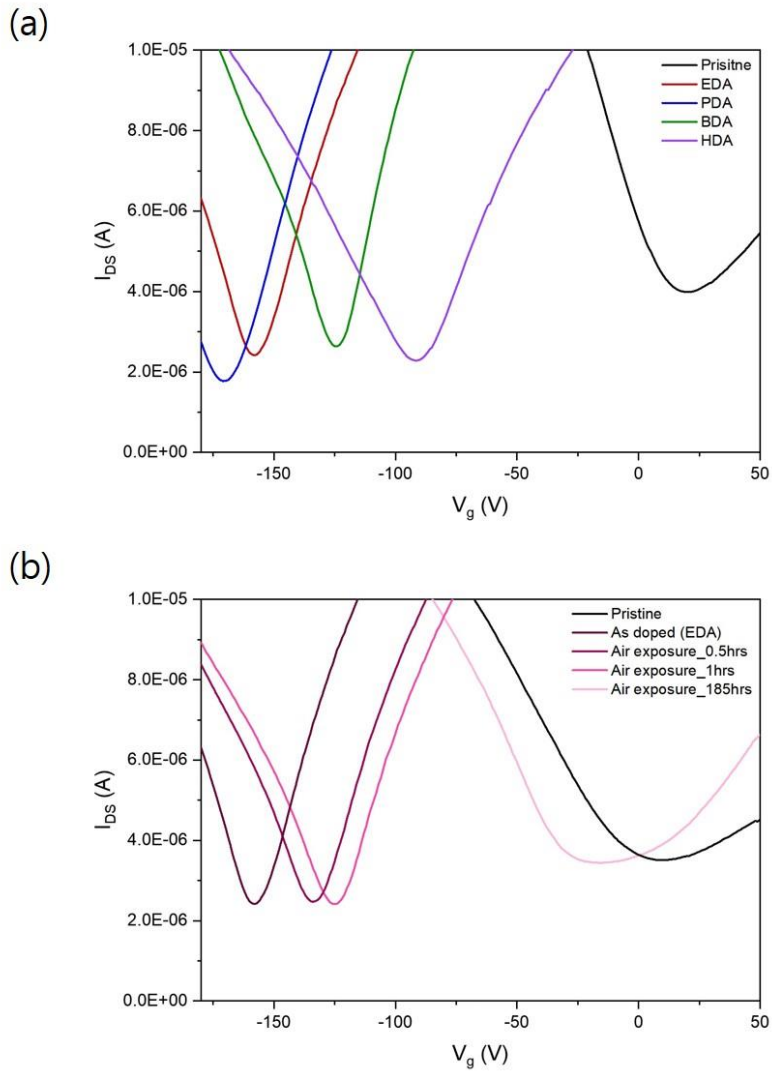


Fig. 2.6. Current-voltage transfer characteristics of graphene doped with aliphatic diamines. (a) Current-voltage characteristics by diamine type, (b) current-voltage characteristics by doping time.

Chapter 3. Paraffin-assisted Graphene Transfer

3.1. Introduction

Since the single layer of graphene is a very thin layer of atomic level, a supporting layer is used to prevent cracks during the transfer process. The support layer commonly used in the wet transfer method is PMMA. Although the process is relatively easy to handle and general process, there is still a problem of quality degradation. [24] The electrical properties are degraded by contamination by polymers that have been incompletely removed after graphene transfer.

Here, we demonstrate novel transfer method using paraffin as supporting layer. When paraffin is used as a supporting layer, heat is applied to coat the graphene. This method is simple compared with the PMMA process in which solid PMMA is dissolved in a solvent to be spin-coated and baked. Since the paraffin is unreactive with graphene, we can achieve graphene with intrinsic characteristics.

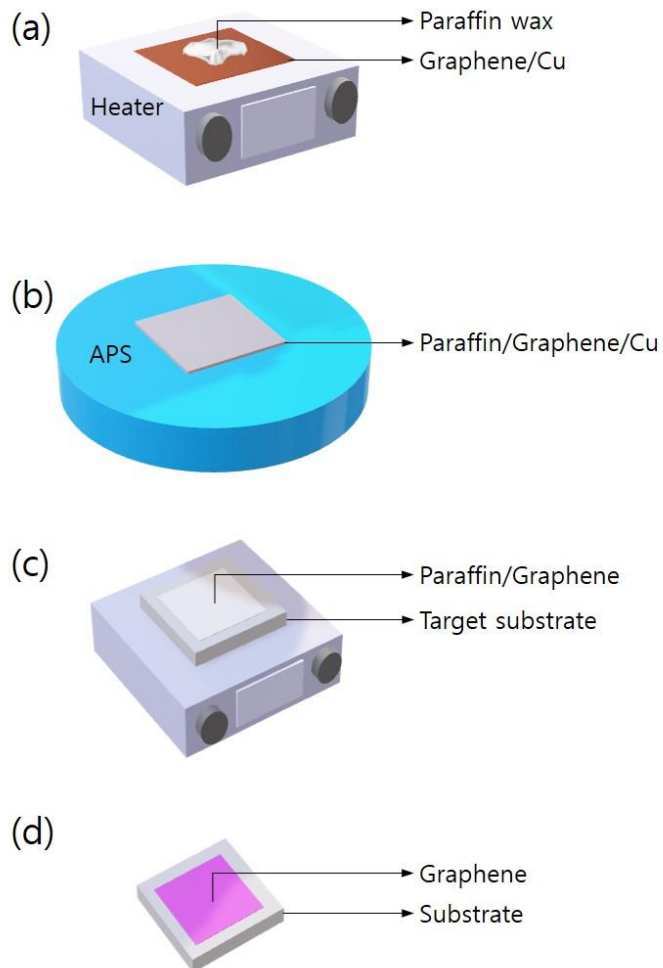


Fig. 3.1. Schematic illustrations of the Paraffin-assisted Graphene Transfer process. (a) Paraffine wax was melted on graphene/Cu, (b) the copper was removed by APS etchant, (c) paraffine-assisted graphene was transferred onto target substrate, (d) paraffin was removed by using toluene.

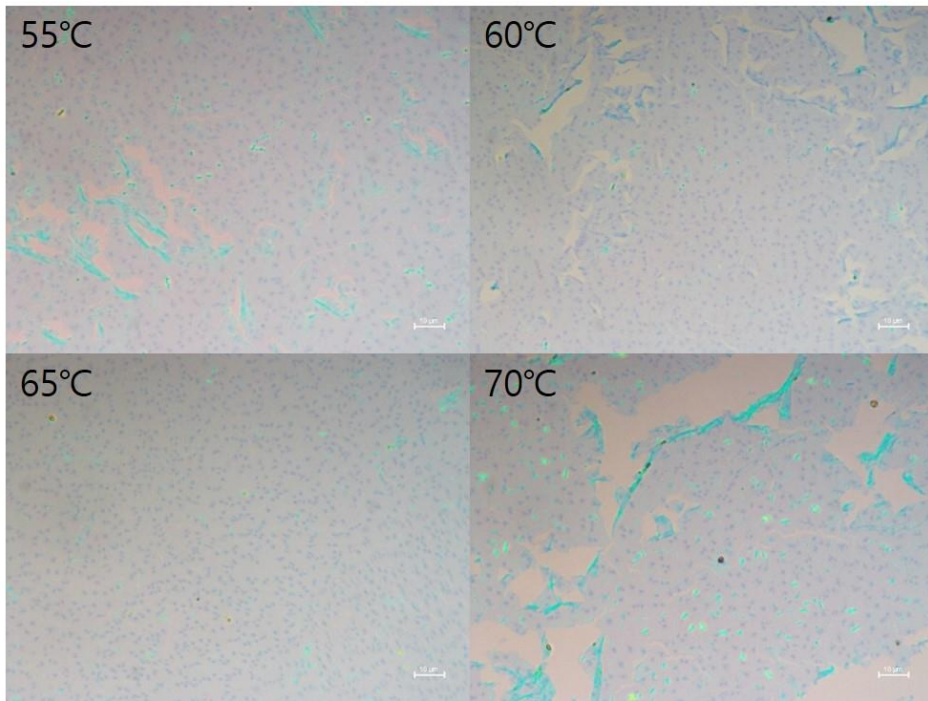


Fig. 3.2. Optical microscope image of the graphene film with paraffin removed after attachment at various temperature.

3.2. Experimental

Chemicals. Paraffin wax (mp 53~58 °C), Poly(methyl methacrylate) (PMMA, $(C_5O_2H_8)_n$), ammonium persulfate $(NH_4)_2S_2O_8$, Toluene (C_7H_8 , 99.8 %) from Sigma-Aldrich; acetone, IPA from Samchun Pure Chemicals; Deionized water from Purescience Ins. was used throughout the experiments.

Paraffin-assisted Graphene Transfer. The transfer process was carried out with commonly used CVD single layer graphene grown on Cu foil. For more information on the CVD graphene synthesis process, refer to chapter 2. The overall flow diagram of the paraffin-assisted transfer process is shown in Fig.3.1. The process of removing the graphene on the backside of the copper foil by RIE is the same as before. Paraffin wax is applied to the upper part of the front side where graphene is left to coat paraffin as a supporting film, and it is heated above the melting point. When the liquid paraffin is uniformly spread, cool it to room temperature. The subsequent copper removal process is the same as mentioned in chapter 2 and after transfer process, the paraffin is removed by immersion in toluene.

Characterization. The graphene film was transferred onto the pre-cleaned SiO_2/Si substrate. After enough drying, the supporting layer was removed with solvent. Optical microscope images were observed with these samples and graphene characteristics were analyzed through Raman spectroscopy. This performed using a Renishaw 2000. The laser excitation wavelength was 514 nm.

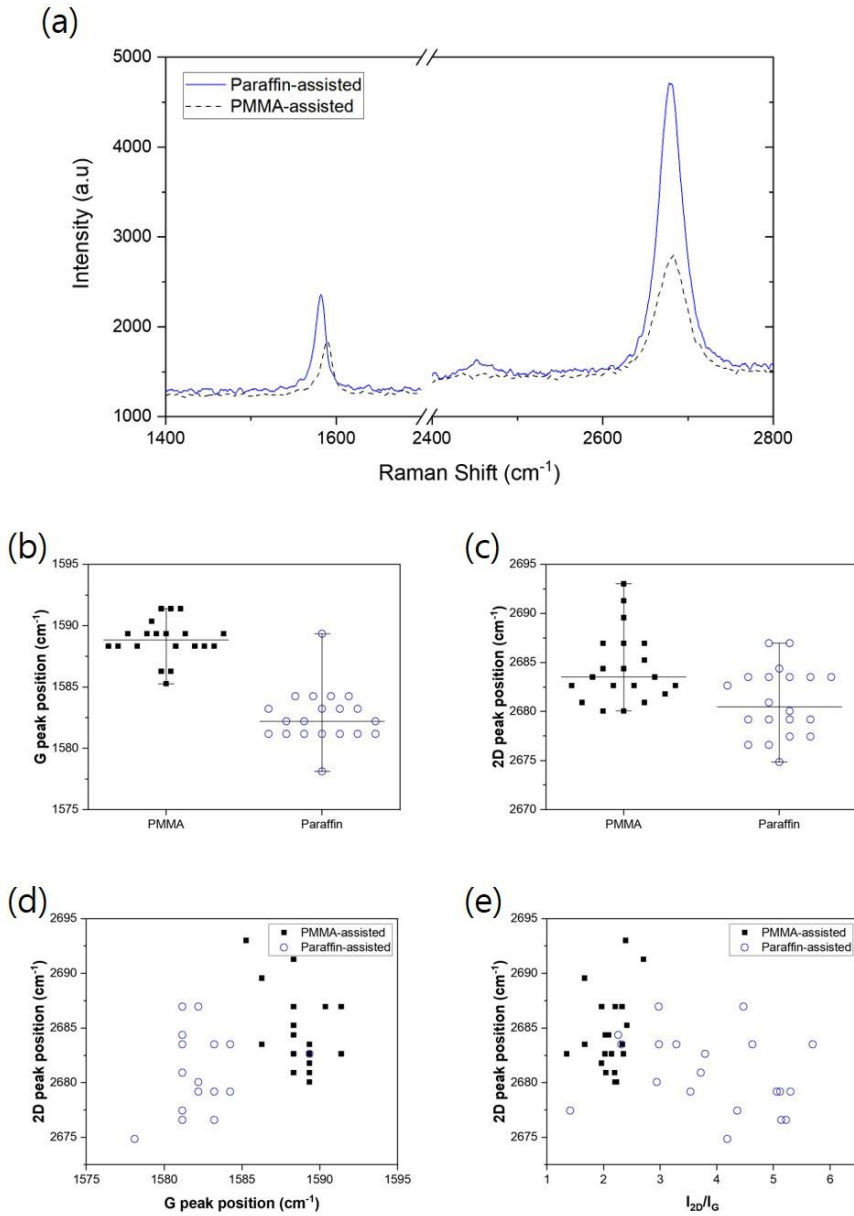


Fig. 3.3. Comparison of Raman spectra for graphene transferred onto the SiO₂/Si substrate. (a) Representative Raman spectra of graphene transferred by paraffin, (b) G peak position, (c) 2D peak position, (d) 2D peak position versus G peak position, (e) 2D peak position versus I_{2D}/I_G ratio.

3.3. Results and Discussion

To optimize the paraffin transfer process, various temperatures were tested for attaching the paraffin-supported graphene to the substrate. Fig. 3.2. shows the optical microscope image of the graphene film with paraffin removed after attachment at various temperature. The optimized temperature was about 65 °C. Below this temperature, there was a portion that could not be transferred due to this surface morphology. And it moved to an unstable form due to the rapidly liquefied paraffin at a temperature higher than this temperature.

Raman spectra were analyzed to compare the characteristics according to the supporting film (Fig. 3.3.). Both PMMA-assisted and paraffin assisted transferred graphene showed a different in intensities of their peaks. The quality of graphene was evaluated by calculating the ratio of I_{2D}/I_G . In Fig. 3.3e, graphene transferred by paraffin-assisted method shows a higher ratio of I_{2D}/I_G as compared to PMMA assisted transfer method. Also, comparing the position shift of G peak with 2D peak, the paraffin-assisted transfer method is the preferred method for achieving good graphene.

Chapter 4. Multi-Stacked Graphene Pellicle for Extreme Ultra Violet Lithography

4.1. Introduction

In order to advance the chip scaling of semiconductor devices, it is required to improve the exposure technique and the technique is being developed in the direction of implementing a fine pattern by reducing the wavelength of the light source. [1] Fig. 4.1. shows the chip scale down trend and lithography tool changes. The resolution limit of the Lithography tool is proportional to the wavelength. Extreme ultraviolet (EUV) exposure, the next generation technology, is the most promising technology to achieve fine patterns in a single resist process.

In EUV lithography tool, light cannot reach the wafer by conventional methods because of the EUV characteristics absorbed by most materials. Therefore, the EUV lithography tool consists of four or more mirrors. When the light emitted from the light source is focused by the condensing lens and enters the mask, the reflected light enters the projection optical system. (Fig. 4.2.) The method of shooting light onto a mask with a circuit drawn and collecting the passing light and repetitively taking patterns on the wafer is the same. However, EUV uses reflected light. This leads to a major difference in the configuration of the tool. [3-4]

Although companies have declared mass production using EUV in 2018, there are some outstanding issues with this technology. Technological issues in application of extreme ultraviolet technology are light source power, resist, and pellicle. [25] Among them, we paid attention to pellicle related problems. The

pellicle prevents the contaminants produced during the exposure process from being transferred into the embodied pattern and is directly related to product yield. Extreme ultraviolet light sources with a wavelength of 13.5 nm have 14 times more photon energy than argon fluoride (ArF) exposure techniques using a 193 nm wavelength. Therefore, it is necessary to develop a new pellicle capable of achieving (1) thermal loads, (2) transmission rate, and (3) productivity in EUV technology since conventional pellicle cannot be applied.

Polycrystalline silicon and silicon nitride thin films are used as prototype pellicle materials in the extreme ultraviolet process under development. However, heat load, permeability and productivity are not satisfied at all. Graphene is attracting attention as a next-generation material to overcome this. It is expected that the permeability of 90 % or more can be achieved by applying the carbon-based film-like pellicle such as graphene as suggested in the roadmap proposed by ASML of maker of extreme ultraviolet exposure equipment. An important development direction in the development of graphene pellicles is the technique of growing graphene on a large area and the technique of stacking graphene through a transfer process with a required size (132 * 104 mm²)

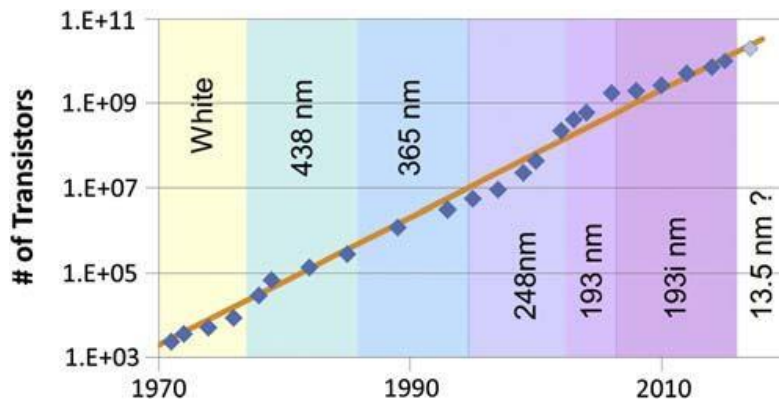


Fig. 4.1. Chip Scale-down and lithography wavelength. The light source used in the 2010s is ArF-immersion at 193 nm wavelength, and A new technology, EUV, uses a wavelength of 13.5 nm. Adapted from *Materials and Processes for Next Generation Lithography*.

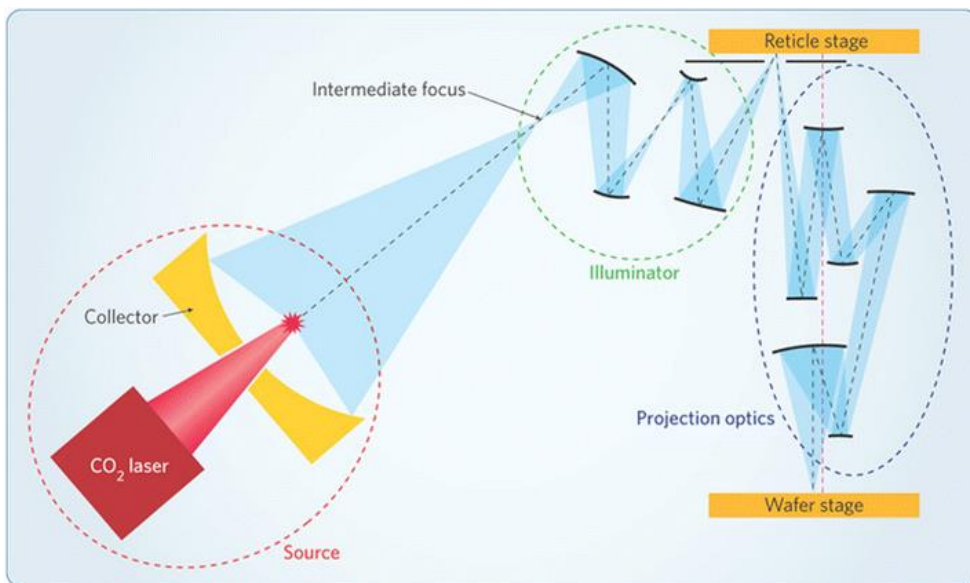


Fig. 4.2. Schematic of EUV lithography system. Light sources delivering hundreds of watts to wafer. Lithography optics focus the reflected light onto a chip. Schematically simple, but real systems are large and complex. [1]

4.2. Experimental

Synthesis of CVD Graphene. Graphene was grown on polycrystalline Cu foil (99.7 %) with hydrogen (15 sccm) and methane (100 sccm) for 30 min at 1000 °C under low pressure (0.76 Torr) in a quartz tube. The annealing time including temperature rise was 1 hour under hydrogen (15 sccm). After the growth time, the furnace was cooled down to room temperature with hydrogen (15 sccm). The graphene on frontside of Cu foil was coated with Poly (methyl methacrylate) (PMMA, $(C_5O_2H_8)_n$) and the graphene on backside was etched by oxygen reactive ion etching (RIE). The Cu foil was removed by Cu etchant (0.1 M ammonium persulfate). For analysis, the graphene floating on deionized water was transferred to a substrate such as silicon wafer, and then PMMA was removed with acetone.

Preparation of multi-stacked graphene film. To fabricate multi-stacked graphene film, conventional wet transfer processes were repeatedly performed. During the Cu wet etching, the removal was practiced for enough time to leave no residue, and rinsing was repeated several times in the deionized water. Fig. 4.3. shows schematic illustrations of graphene stacking process.

Characterization of multi-stacked graphene film. UV-Vis, AFM and Raman were used to characterize multi-stacked graphene films that had undergone ten repetitive stacking processes. For AFM and Raman analysis, multi-stacked graphene film was transferred onto SiO_2/Si substrates and dried. Transmittance analysis in the visible region was analyzed with multi-stacked graphene sample transferred onto PET.

Fabrication of free-standing multi-stacked graphene sample. EUV

transmittance was obtain by FST company. Due to the nature of the EUV light that generates a high thermal load in a vacuum environment, it was impossible to proceed in the state of being transferred onto PET. Free-standing samples were prepared in a circle with a diameter of 10 mm or more. First, a multi-stacked graphene film with PMMA was transferred onto a cleaned holder material by wet transfer method. The sample was completely dried for more than 48 hours in an isolated and stable environment at room temperature to remove moisture before the next process. After sufficient drying, the supporting PMMA was removed. In the process of dissolving and removing PMMA with solvent, a separate process has been devised so that the sample can be held without external disturb. (Fig. 4.4a) At the slowest and most stable rate, the sample was placed vertically into the solvent. The PMMA settled in toluene for 30 minutes, then lifted vertically and dried. The sample was dried for 48 hours or more in an environment free from external interference and finally achieved a free-standing sample. (Fig. 4.4b)

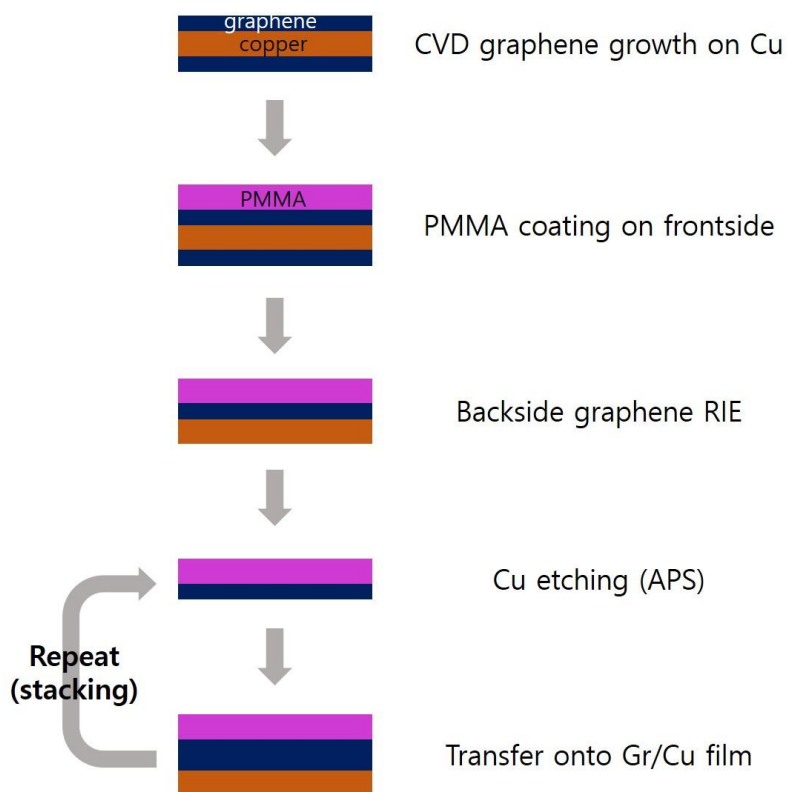


Fig. 4.3. Schematic of the graphene stacking process. Multi-stacked graphene film was made by conventional wet transfer method on the CVD graphene.

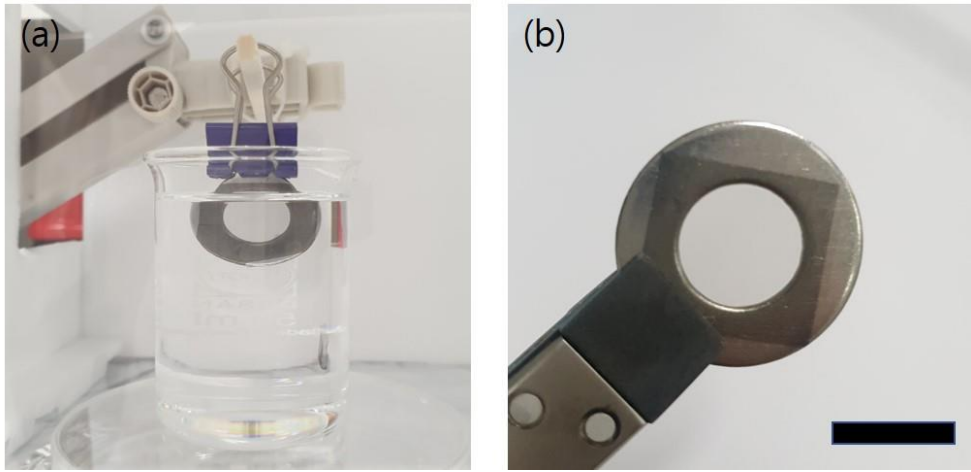


Fig. 4.4. Fabrication process of free-standing sample. (a) Removal of PMMA by using toluene at clean and stable room. The sample was soaked vertically and then held up and dried. (b) a 15.4 nm thickness free-standing multi-stacked graphene film with inner diameter of 10 mm. (scale bar = 10 mm)

4.3. Results and Discussion

The transmittance of the visible region measured by UV-Vis was 77.4 % for a multi-stacked graphene film with 10 repeated stacking processes. (Fig. 4.5a). This value is consistent with a reduction in transmittance about 2.3 % per graphene reported previously. [26] The thickness of the sample confirmed by AFM was 15.4 nm. As shown in Fig. 4.6., the changes of peak positions and intensities was observed as the number of stacking of graphene increased. As the number of transfer increases, the ratio of I_{2D}/I_G decreases (Fig. 4.6e)

We demonstrated free-standing samples of thinner graphene film than in previous studies. EUV transmittance of this sample was 87 %.

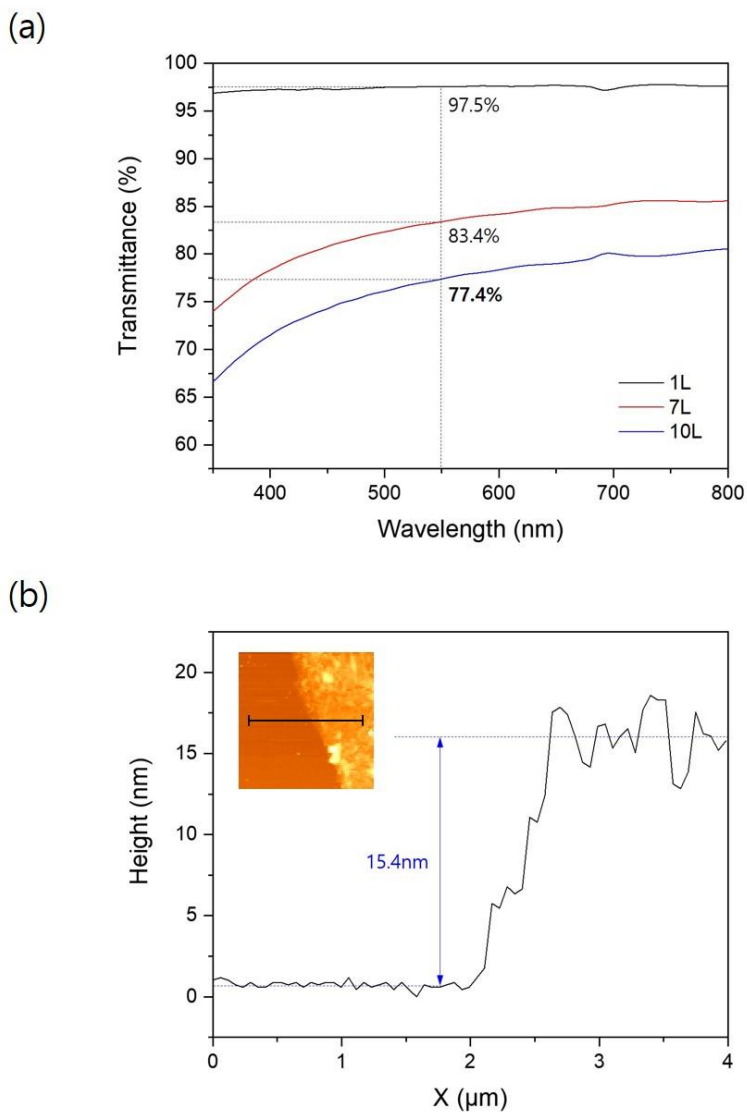


Fig. 4.5. Transmittance at visible light, thickness of multi-stacked graphene film. (a) Visible light transmittance of 1 layer (1L), 7 layer (7L) and 10 layer (10L) graphene films. (b) Height data of multi-stacked (10L) graphene film measured by AFM. The median thickness of 10L graphene is 15.4 nm.

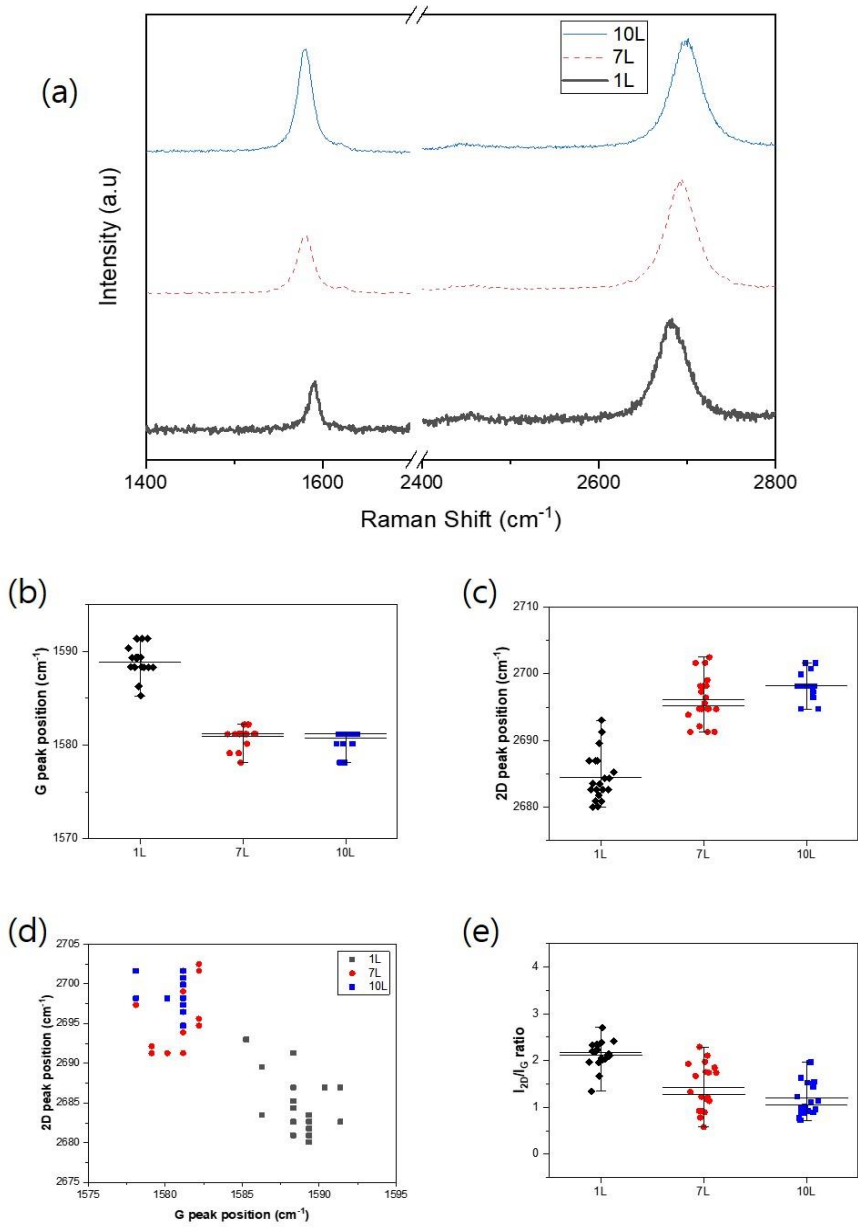


Fig. 4.6. Raman spectra for graphene and multi-stacked graphene onto the SiO₂/Si substrate. (a) Representative Raman spectra of 1 layer, 7 layer and 10 layer graphene film (b) G peak position, (c) 2D peak position, (d) 2D peak position versus G peak position, (e) 2D peak position versus I_{2D}/I_G ratio.

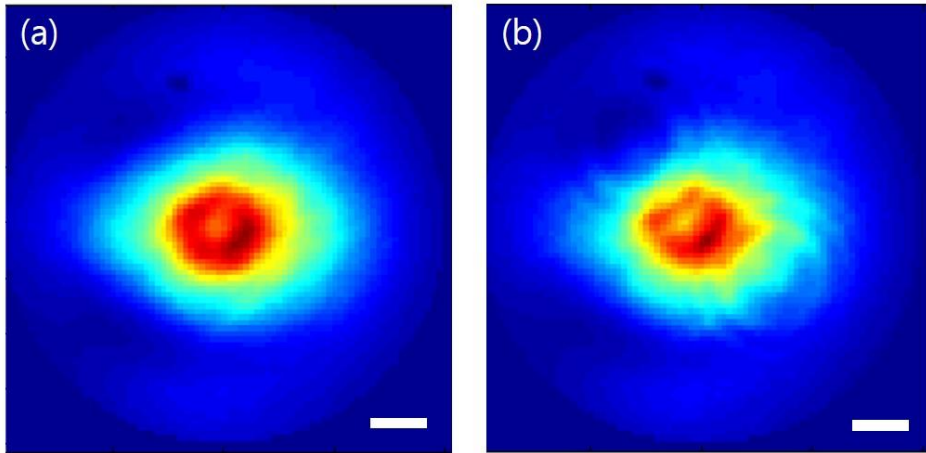


Fig. 4.7. EUV transmission characteristics of multi-stacked graphene film. (a) Reference beam profile on CCD, (b) transmitted beam profile on CCD. EUV transmittance (87 %) of a multi-stacked graphene sample was obtained by comparing (a) and (b). (scale bar = 1 mm)

Chapter 5. Conclusion

In this thesis, we proposed ‘Multi-Stacked Graphene Pellicle’ for EUV lithography. Before the proposal of ‘Multi-Stacked Graphene Pellicle’, a large area graphene film was synthesized by chemical vapor deposition (CVD) method. By the vapor-phase molecular doping and its characteristics can be controlled in a better direction. We also propose a novel transfer method, paraffin-assisted transfer. This method can achieve graphene with better characteristics than conventional transfer method.

The proposed ‘Multi-Stacked Graphene Pellicle’ for EUV lithography must be developed in terms of heat load, transmittance in EUV region and productivity. To meet these requirements, we aimed to develop thin films of several tens of nanometer. The typical wet transfer method was repeated to prepare multi-stacked graphene film corresponding to ten layers. UV-Vis and Raman spectroscopic analysis showed that the transfer and stacking process was completed properly. The thickness of multi-stacked graphene film was measured by atomic force microscope (AFM). And the result was about 15.4 nm. To measure the transmittance in the EUV region multi-stacked graphene film, a free-standing sample of 10 mm in diameter was fabricated. And the EUV light transmittance measured in a vacuum environment 87 %.

Bibliography

1. Wagner, C.; Harned, N., EUV LITHOGRAPHY Lithography gets extreme. *Nat Photonics* **2010**, *4* (1), 24-26.
2. Mackay, R. S., The future of lithography after 193 nm optics. *Microelectron Eng* **1998**, *42*, 71-74.
3. Schafers, F., Multilayers for the EUV/soft X-ray range. *Physica B* **2000**, *283* (1-3), 119-124.
4. Louis, E.; Voorma, H. J.; Koster, N. B.; Bijkerk, F.; Platonov, Y. Y.; Zuev, S. Y.; Andreev, S. S.; Shamov, E. A.; Salashchenko, N. N., Multilayer Coated Reflective Optics for Extreme Uv Lithography. *Microelectron Eng* **1995**, *27* (1-4), 235-238.
5. Hu, Q.; Kim, S. G.; Shin, D. W.; Kim, T. S.; Nam, K. B.; Kim, M. J.; Chun, H. C.; Yoo, J. B., Large-scale nanometer-thickness graphite films synthesized on polycrystalline Ni foils by two-stage chemical vapor deposition process. *Carbon* **2017**, *113*, 309-317.
6. Kim, T. S.; Shin, D. W.; Kim, S. G.; Kim, M. J.; Yoo, J. B., Large area nanometer thickness graphite freestanding film without transfer process. *Chem Phys Lett* **2017**, *690*, 101-104.
7. Kim, I. S.; Kim, J. W.; Oh, H. K., Study of Temperature Behaviors for a Pellicle in Extreme-Ultraviolet Lithography: Mesh Structure. *Jpn J Appl Phys* **2013**,

52 (12).

8. Kim, S. G.; Shin, D. W.; Kim, T.; Kim, S.; Lee, J. H.; Lee, C. G.; Yang, C. W.; Lee, S.; Cho, S. J.; Jeon, H. C.; Kim, M. J.; Kim, B. G.; Yoo, J. B., Large-scale freestanding nanometer-thick graphite pellicles for mass production of nanodevices beyond 10 nm. *Nanoscale* **2015**, *7* (35), 14608-14611.
9. Lee, H. C.; Kim, E. J.; Kim, J. W.; Oh, H. K., Temperature behavior of pellicles in extreme ultraviolet lithography. *J Korean Phys Soc* **2012**, *61* (7), 1093-1096.
10. Shroff, Y. A.; Leeson, M.; Yan, P. Y.; Gullikson, E.; Salmassi, F., High transmission pellicles for extreme ultraviolet lithography reticle protection. *J Vac Sci Technol B* **2010**, *28* (6), C6e36-C6e41.
11. Meyer, J. C.; Geim, A. K.; Katsnelson, M. I.; Novoselov, K. S.; Booth, T. J.; Roth, S., The structure of suspended graphene sheets. *Nature* **2007**, *446* (7131), 60-63.
12. Novoselov, K. S.; Geim, A. K.; Morozov, S. V.; Jiang, D.; Zhang, Y.; Dubonos, S. V.; Grigorieva, I. V.; Firsov, A. A., Electric field effect in atomically thin carbon films. *Science* **2004**, *306* (5696), 666-669.
13. Avouris, P.; Dimitrakopoulos, C., Graphene: synthesis and applications. *Mater Today* **2012**, *15* (3), 86-97.
14. Singh, V.; Joung, D.; Zhai, L.; Das, S.; Khondaker, S. I.; Seal, S., Graphene based materials: Past, present and future. *Prog Mater Sci* **2011**, *56* (8),

1178-1271.

15. Somani, P. R.; Somani, S. P.; Umeno, M., Planer nano-graphenes from camphor by CVD. *Chem Phys Lett* **2006**, *430* (1-3), 56-59.

16. Li, X. S.; Cai, W. W.; Colombo, L.; Ruoff, R. S., Evolution of Graphene Growth on Ni and Cu by Carbon Isotope Labeling. *Nano Lett* **2009**, *9* (12), 4268-4272.

17. Kim, K. S.; Zhao, Y.; Jang, H.; Lee, S. Y.; Kim, J. M.; Kim, K. S.; Ahn, J. H.; Kim, P.; Choi, J. Y.; Hong, B. H., Large-scale pattern growth of graphene films for stretchable transparent electrodes. *Nature* **2009**, *457* (7230), 706-710.

18. Li, X. S.; Cai, W. W.; An, J. H.; Kim, S.; Nah, J.; Yang, D. X.; Piner, R.; Velamakanni, A.; Jung, I.; Tutuc, E.; Banerjee, S. K.; Colombo, L.; Ruoff, R. S., Large-Area Synthesis of High-Quality and Uniform Graphene Films on Copper Foils. *Science* **2009**, *324* (5932), 1312-1314.

19. Gupta, A.; Chen, G.; Joshi, P.; Tadigadapa, S.; Eklund, P. C., Raman scattering from high-frequency phonons in supported n-graphene layer films. *Nano Lett* **2006**, *6* (12), 2667-2673.

20. Obradovic, B.; Kotlyar, R.; Heinz, F.; Matagne, P.; Rakshit, T.; Giles, M. D.; Stettler, M. A.; Nikonov, D. E., Analysis of graphene nanoribbons as a channel material for field-effect transistors. *Appl Phys Lett* **2006**, *88* (14).

21. Liu, H. T.; Liu, Y. Q.; Zhu, D. B., Chemical doping of graphene. *J Mater*

Chem **2011**, *21* (10), 3335-3345.

22. Jo, I.; Kim, Y.; Moon, J.; Park, S.; Moon, J. S.; Park, W. B.; Lee, J. S.; Hong, B. H., Stable n-type doping of graphene via high-molecular-weight ethylene amines. *Phys Chem Chem Phys* **2015**, *17* (44), 29492-29495.

23. Kim, Y.; Ryu, J.; Park, M.; Kim, E. S.; Yoo, J. M.; Park, J.; Kang, J. H.; Hong, B. H., Vapor-Phase Molecular Doping of Graphene for High-Performance Transparent Electrodes. *Acs Nano* **2014**, *8* (1), 868-874.

24. Lin, Y. C.; Lu, C. C.; Yeh, C. H.; Jin, C. H.; Suenaga, K.; Chiu, P. W., Graphene Annealing: How Clean Can It Be? *Nano Lett* **2012**, *12* (1), 414-419.

25. Brouns, D., Development and performance of EUV pellicles. *Adv Opt Technol* **2017**, *6* (3-4), 221-227.

26. Nair, R. R.; Blake, P.; Grigorenko, A. N.; Novoselov, K. S.; Booth, T. J.; Stauber, T.; Peres, N. M. R.; Geim, A. K., Fine structure constant defines visual transparency of graphene. *Science* **2008**, *320* (5881), 1308-1308.

국 문 초 록

집적회로의 기술이 발전함에 따라서 트랜지스터의 선폭을 감소시키는 것은 필연적인 일이다. 선폭의 감소를 위해서는 다양한 반도체 공정 기술의 개발이 필요하며, 그 중에서도 노광 기술은 특히 주목을 받고 있다. 수 백 나노미터 수준의 파장을 이용하는 원자외선 (DUV) 노광 기술은 한계에 도달하였으며, 새로운 기술로서 더 낮은 파장 영역을 사용하는 극자외선 (EUV) 노광 기술의 도입이 시작되었다. 이 때 사용되는 13.5nm의 EUV 영역의 빛은 고밀도 플라즈마로부터 형성되며, 그에 따라 기존의 원자외선 노광과는 달리 진공의 환경에서 공정이 진행되어야 한다. 이러한 차이점은 새로운 광학 시스템을 필요로 할 뿐만 아니라, 펠리클을 포함한 레티클 재료의 개발을 필요로 한다.

본 연구에서는 적층 그래핀 펠리클을 제안한다. 탄소의 동소체이며 원자들이 2차원 평면으로 sp^2 혼성 결합의 구조를 이루고 있는 그래핀은 원자 단일층의 두께를 지니기 때문에 뛰어난 특성들을 나타낸다. 이 중에서도 극자외선 노광 기술용 펠리클에 응용될 수 있는 이유는 전기적 특성, 열적 특성, 빛을 투과시키는 광학적 특성 그리고 대면적으로 유지될 수 있는 기계적 강도 특성까지 뛰어나기 때문이다.

적층 그래핀 펠리클의 제안에 앞서서 먼저, 대면적으로 화학기상증착법(chemical vapor deposition)을 이용하여 대면적으로 그래핀 박막을 합성하였다. 화학기상증착법으로 합성된 그래핀에 기체상 분자 도핑

(vapor-phase molecular doping)을 하여 그 특성을 더 뛰어난 방향으로 조절할 수 있음을 확인하였다. 또한 파라핀을 이용하는 새로운 전사 방법을 제안하였으며 이 방법으로 기존의 전사방법보다 좋은 특성의 그래핀을 확인할 수 있었다.

극자외선 노광 기술에 적층 그래핀 펠리클을 적용하기 위해서는 열 부하, 투과율 그리고 생산성 관점에서 개발되어야 한다. 이를 위해서 수십 나노미터 수준의 박막을 구현하는 것을 목표로 연구가 진행되었다. 일반적인 습식전사 방법을 반복하여 열 층에 해당하는 적층 그래핀 박막을 준비하였다. 자외선 분광 분석 및 라만 분광 분석으로 적층이 제대로 이루어졌음을 확인했으며, 원자현미경으로 형성된 적층 박막의 두께서 약 15.4nm였다. 적층 그래핀 박막으로 극자외선 영역에서의 투과율을 측정하기 위하여 지름 10mm에 해당하는 원의 크기로 독립형 (free-standing) 박막 시료를 구현하는 데에 성공하였으며, 진공의 환경에서 측정된 극자외선 투과율은 87%였다.

주요어: 극자외선 노광, 적층 그래핀 펠리클, 극자외선 투과율 측정, 화학 기상증착법, 파라핀 기반의 전사 방법

학번: 2017-29383

감사의 글

관악산에서 지내면서 고민하고 연구했던 지난 날들에 도움을 주셨던 모든 분들께 감사함을 전합니다.

석사과정 기간동안 지도해주신 홍병희 교수님께 말로 표현하기에도 부족한 감사와 존경을 표합니다. 교수님의 지도 아래서 연구를 하였던 지난 시간들은 영광이었습니다. 졸업 후에도 부끄럽지 않은 제자가 되기 위해서 제 자리에서 최선을 다하겠습니다.

그래핀 연구실의 선후배들에게 항상 고맙습니다. 덕분에 고루하지 않은 스스로가 될 수 있었고 지난 시간들을 즐겁게 보냈습니다. 연구에 대한 고민으로 힘든 나날들이라도 행복하게 보내기를, 꿈꾸고 원하는 내일을 맞이하기를 바랍니다.

학술연수의 기회를 가질 수 있도록 응원해주신 회사의 선배님들께 감사의 말씀을 전합니다. 학교에 있었던 부재의 시간동안 선배님들의 고마움과 소중함을 느꼈습니다. 돌아가서는 더 좋은 선배, 동료 그리고 후배가 되도록 노력하겠습니다.

힘들 때면 곁에서 위안이 되어주었던 친구들에게도 고마움을 전합니다. 외로울 수 있었던 봉천동에서 좋은 추억들을 만들어주어서 고맙습니다.

나의 버팀목, 가족들에게 무엇보다 큰 감사와 사랑을 전합니다.

2019년 여름, 김은정 드림